Available online at www.sciencedirect.com
SCIENCE DIRECT
Journal of Power Sources 156 (2006) 560–566
JOURNAL OF POWER SOURCES
www.elsevier.com/locate/jpowsour

Solid-state Li/$LiFePO_4$ polymer electrolyte batteries incorporating an ionic liquid cycled at 40 °C

Joon-Ho Shin, Wesley A. Henderson, Silvera Scaccia, Pier Paolo Prosini, Stefano Passerini *

ENEA (Italian National Agency for New Technologies, Energy and the Environment), IDROCOMB, Via Anguillarese 301, 00060 Rome, Italy

Received 21 December 2004; received in revised form 18 May 2005; accepted 3 June 2005
Available online 18 August 2005

Abstract

The cycle behaviour and rate performance of solid-state Li/$LiFePO_4$ polymer electrolyte batteries incorporating the *N*-methyl-*N*-propylpyrrolidinium bis(trifluoromethanesulfonyl)imide (PYR_{13}TFSI) room temperature ionic liquid (IL) into the $P(EO)_{20}$LiTFSI electrolyte and the cathode have been investigated at 40 °C. The ionic conductivity of the $P(EO)_{20}$LiTFSI + PYR_{13}TFSI polymer electrolyte was about 6×10^{-4} S cm^{-1} at 40 °C for a PYR_{13}^+/Li^+ mole ratio of 1.73. Li/$LiFePO_4$ batteries retained about 86% of their initial discharge capacity (127 mAh g^{-1}) after 240 continuous cycles and showed excellent reversible cyclability with a capacity fade lower than 0.06% per cycle over about 500 cycles at various current densities. In addition, the Li/$LiFePO_4$ batteries exhibited some discharge capability at high currents up to 1.52 mA cm^{-2} (2 C) at 40 °C which is very significant for a lithium metal-polymer electrolyte (solvent-free) battery systems. The addition of the IL to lithium metal-polymer electrolyte batteries has resulted in a very promising improvement in performance at moderate temperatures.

Keywords: Polymer electrolyte; Ionic liquid; Lithium battery; Ionic conductivity; $LiFePO_4$

1. Introduction

Rechargeable lithium metal-polymer batteries (LMPBs) have been considering as the most probable next generation of power sources for portable electronic devices, telecommunication equipment and hybrid electric vehicles (HEVs) because of their high energy density and design flexibility [1]. Much effort has been devoted to the discovery (or development) of new cathode materials. Extensive research on polymer electrolytes has also been performed worldwide over the last few decades. Several approaches have been proposed to enhance the ionic conductivity of lithium-conducting polymer electrolytes. The addition of aprotic solvents such as ethylene carbonate (EC) and propylene carbonate (PC) into conventional polymer electrolytes has successfully improved their ionic conductivity [2,3], but this also causes severe compatibility problems with the reactive lithium metal anode.

Presently, a very promising approach appears to be the incorporation of ionic liquids (ILs) into PEO-based electrolytes [4–7]. Although the phenomenon is not yet understood, the lithium transport mechanism in the polymer electrolytes is found to be strongly enhanced by the presence of certain ionic liquids. Electrolytes containing ILs are gaining increased notoriety [4,8–10]. The interest in these materials arises from their desirable properties such as non-volatility, non-flammability, high thermal stability and high conductivity [11,12]. Most of the research work has been focused on ILs based upon imidazolium cations. These ILs do tend to have a low viscosity and high ionic conductivity [13–15], but also show poor stability towards Li metal (due to the reactivity of the acidic protons on the cation) [16,17]. On the other hand, ILs consisting of *N*-alkyl-*N*-methylpyrrolidinium cations and

* Corresponding author. Tel.: +39 06 3048 4985; fax: +39 06 3048 6357.
E-mail address: passerini@casaccia.enea.it (S. Passerini).

0378-7753/$ – see front matter © 2005 Elsevier B.V. All rights reserved.
doi:10.1016/j.jpowsour.2005.06.026

bis(trifluoromethanesulfonyl)imide anions not only have a relatively high ionic conductivity, but also a wide electrochemical stability window [4,18]. In a previous paper [4], we demonstrated that the combination of *N*-methyl-*N*-propylpyrrolidinium bis(trifluoromethanesulfonyl)imide ($PYR_{13}TFSI$) and $P(EO)_{20}LiTFSI$ resulted in free-standing, easy to handle, membranes which have a high conductivity at moderate temperatures. It is important to note that these are homogeneous solid polymer electrolytes (consisting solely of commercial PEO and two salts) rather than gel electrolytes. There is no liquid-phase present which may weep from the polymer electrolyte when pressure is applied. It was found that Li/V_2O_5 batteries with such polymer electrolytes containing the IL show a high specific capacity and low capacity fade during cycling at moderate or low temperatures. In this study we report further on the performance of solid-state $Li/P(EO)_{20}LiTFSI + PYR_{13}TFSI/LiFePO_4$ batteries at 40 °C. The results presented in this work are very good with respect to the state of the art in lithium metal-polymer electrolyte (solvent-free) battery systems [19] that operate at temperatures above 60 °C. IL containing PEO-based electrolytes are a promising approach for the realization of lithium metal-polymer electrolyte batteries operating at ambient and perhaps even sub-ambient temperatures.

$LiFePO_4$ was selected as a cathode because of its low cost, abundance and environmentally benignity compared to conventional transition metal oxides, $LiMO_2$ (M = Ni, Mn and Co). $LiFePO_4$ has been shown to have an excellent performance in Li secondary batteries based upon both polymer electrolytes [20] and liquid electrolytes [21]. $LiFePO_4$ was synthesized through an energy saving, sol–gel procedure [22] that requires very short and moderate temperature heat treatments.

2. Experimental

2.1. Materials

PEO ($M_w = 4 \times 10^6$, Union Carbide) and LiTFSI ($LiN(SO_2CF_3)_2$, a gift from 3M) were dried under vacuum for 48 and 24 h at 50 and 180 °C, respectively. Carbon (electronic conductor, KJB, Akzo Nobel) was dried under vacuum at 150 °C and sieved (400 mesh sieve). 1-Methylpyrrolidine (97%) and 1-iodopropane (99%) were purchased from Aldrich and used as received.

2.2. $PYR_{13}TFSI$ preparation

$PYR_{13}I$ was prepared by the reaction of 1-methylpyrrolidine with a stoichiometric amount of 1-iodopropane in ethyl acetate. The resulting $PYR_{13}I$ salt was washed several times with ethyl acetate and then recrystallised by dissolving/melting the salt in hot acetone and adding ethyl acetate to obtain a pure white salt. Combining $PYR_{13}I$ and LiTFSI (1:1 mol ratio) in deionized H_2O gave $PYR_{13}TFSI$ (the aqueous layer containing the LiI and the IL phase separated). The aqueous phase was removed and the salt was washed five times with deionized H_2O to remove residual LiI. The final aqueous layer was removed and the $PYR_{13}TFSI$ was heated to high temperature on a hot plate to remove trace solvents. Activated carbon (Darco-G60, Aldrich) was added and the hot mixture was stirred on a hot plate overnight. Acetone was added and the mixture was filtered through a short-activated alumina (acidic, Brockmann I, Aldrich) column. The acetone was removed by heating and the $PYR_{13}TFSI$ was dried under high vacuum at 100 °C overnight and then at 120 °C for 6 h. The resulting $PYR_{13}TFSI$ is a clear, colorless liquid at room temperature. The IL was stored and handled in a dry room (<0.2% relative humidity, 20 °C).

2.3. $P(EO)_{20}LiTFSI$ + IL preparation

The polymer electrolyte with the IL, $P(EO)_{20}LiTFSI + x\ PYR_{13}TFSI$ ($x = PYR_{13}^+/Li^+$ mole fraction), was prepared by a hot-pressing technique. The PEO and LiTFSI were first mixed in a mortar (EO/Li = 20) and then the $PYR_{13}TFSI$ was added. The mixture was vacuum-sealed in a coffee bag-like envelope and annealed at 90 °C overnight to homogenize it. A free-standing polymer electrolyte film was obtained by hot-pressing the resulting mixture between Mylar sheets (Dupont, polyester, 100 μm thick) at 110 °C for approximately 20 min. No solvent was used during the electrolyte preparation. The final solid-state solvent-free $P(EO)_{20}LiTFSI + 1.73\ PYR_{13}TFSI$ polymer electrolyte has a thickness of about 100 μm [5].

2.4. $LiFePO_4$ cathode preparation

$LiFePO_4$ was synthesized following an energy saving procedure developed at ENEA [22]. Briefly, amorphous $FePO_4$ was obtained by spontaneous precipitation from equimolar aqueous solutions of $Fe(NH_4)_2(SO_4)_2{\cdot}6H_2O$ and $NH_4H_2PO_4$, using hydrogen peroxide as an oxidizing agent. Amorphous $LiFePO_4$ was then obtained by chemical lithiation of the $FePO_4$. Finally, crystalline $LiFePO_4$ was obtained by heating the amorphous compound at 550 °C for 60 min under a reducing atmosphere (5% H_2/Ar). The final material contains about 2 at.% of trivalent iron (Fe^{3+}) [23] that reduces the specific capacity to 154 mAh g^{-1}.

Composite cathodes consisting of $LiFePO_4$ (43 wt.%), PEO ($M_w = 4 \times 10^6$, 17.5 wt.%), LiTFSI (5 wt.%), PYR_{13}TFSI (27.5 wt.%) and carbon (7 wt.%) were prepared in a manner similar to the polymer electrolyte. First, $LiFePO_4$ and carbon were mixed by ball milling with glass balls in a plastic bottle for 12 h. PEO was added and the mixture was ball-milled for another 12 h. LiTFSI and $PYR_{13}TFSI$ were added to the mixture followed by mixing in a mortar. The mixture was then vacuum sealed in a coffee bag-like envelope and annealed at 90 °C overnight. The preliminary cathode films were made by hot-pressing the resulting mixture at room temperature. Thin cathode films (ca. 45 μm thick) were finally

obtained by calendaring the preliminary cathode films placed between two Mylar sheets at room temperature. No solvent was used during the composite cathode preparation. The cathode used in battery assembly was a disc with a surface area of 0.8 cm^2.

2.5. Battery assembly and instrumentation

The batteries were assembled by sandwiching the polymer electrolyte films between a Li metal anode (50 μm thick) and a composite cathode film [4]. The assembled cells were vacuum-sealed in coffee bag-like envelopes and laminated twice by hot-rolling at 100 °C. Cu (50 μm thick) and Al foils were used as current collectors for the anode and cathode, respectively. All batteries were thermally equilibrated for about 1 h at the selected operating temperature (40 °C) prior to measurements. The batteries were cycled under constant current and/or constant voltage. The battery cycle tests were performed between 2 and 4 V using a Maccor battery cycler (S4000).

3. Results and discussion

Fig. 1 reports a few selected cycles of a Li/$P(EO)_{20}$LiTFSI + IL/$LiFePO_4$ cell cycled at 40 °C and a moderate rate (0.05 C) at 100% depth of discharge (DOD). The results clearly show the good performance in terms of capacity and reversibility for the polymer electrolyte (solvent-free) battery. In the first cycle, the cell delivered 148 mAh g^{-1} (based on the active material mass) corresponding to 96.1% of the nominal capacity (154 mAh g^{-1}). The average voltage during the charge and discharge plateaus in the first cycles is about 3.5 and 3.4 V, respectively, i.e., within 100 mV. Upon cycling for more than 6 months, the two plateaus shortened and shifted only slightly. The shift was limited to approximately 70 mV over the entire cycling test. Overall, the cell showed a lower change in performance than Li/$LiFePO_4$ cells with typical electrolytes such as an EC/DMC-$LiPF_6$ liquid electrolyte [24,25] or $P(EO)_{35}LiCF_3SO_3$ polymer electrolyte [20].

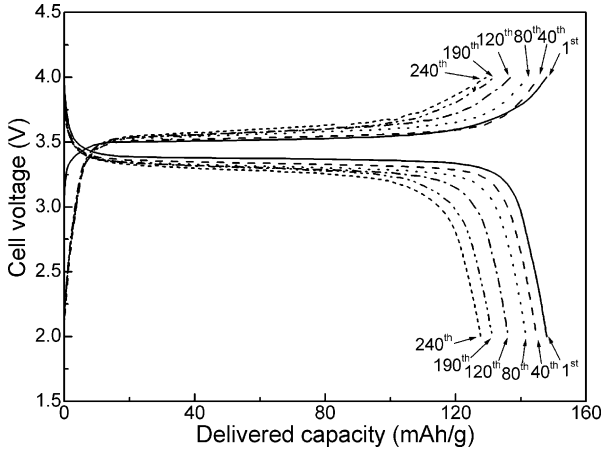

Fig. 1. Voltage profile of a Li/$P(EO)_{20}$LiTFSI + IL/$LiFePO_4$ cell at 40 °C. Active material loading: 4.9 mg cm^{-2}; charge and discharge current: 0.042 mA cm^{-2} (0.05 C).

Fig. 2 demonstrates the performance of the Li/$P(EO)_{20}$ LiTFSI + IL/$LiFePO_4$ cells. Upon continuous cycling, the delivered capacity (Fig. 2a) decreased from the initial 148 to 127 mAh g^{-1} at the 240th cycle, corresponding to 82.7% of the nominal capacity and 85.7% capacity retention. Throughout the entire cycle test, the cell discharge/charge efficiency was always close to unity (Fig. 2b). More precisely, its average value was 0.992. The overall capacity fading over about 240 cycles (Fig. 2b) was about 14% of the initial capacity corresponding to an average capacity fading only slightly higher than 0.056% per cycle or 0.086 mAh g^{-1} per cycle. A comparison with work from other groups shows that the fading in our cells is lower than that of IL-free Li/$LiFePO_4$ polymer batteries tested at 0.2 mA cm^{-2} and 100 °C (0.17% per cycle) [20] and that recently reported (0.31% per cycle) for a Li/$LiFePO_4$ cell with an EC/dimethyl carbonate (DMC)-$LiPF_6$ liquid electrolyte [24] after 60 cycles.

Fig. 3 illustrates the dependence of the delivered capacity of a Li/$P(EO)_{20}$LiTFSI + IL/$LiFePO_4$ cell at 40 °C

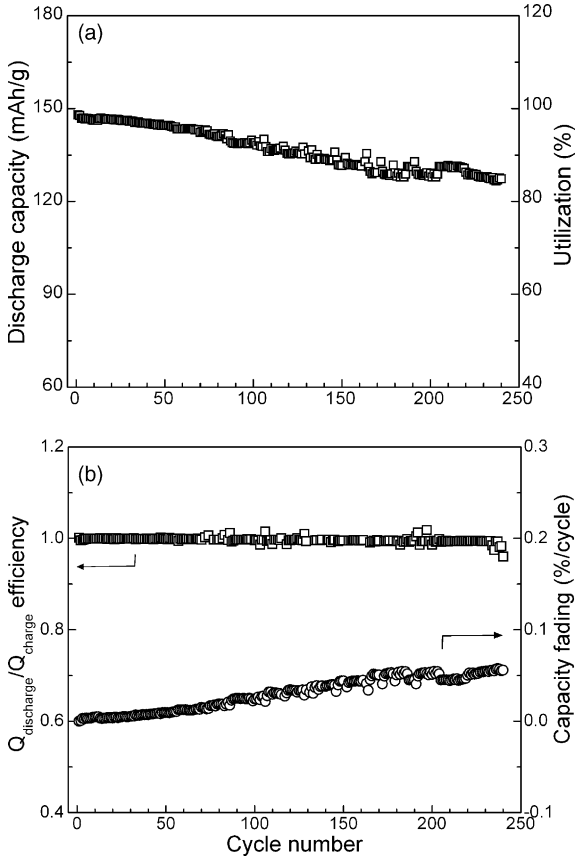

Fig. 2. Cycling performance of a Li/$P(EO)_{20}$LiTFSI + IL/$LiFePO_4$ cell at 40 °C: (a) discharge capacity and active material utilization; (b) discharge/charge efficiency and capacity fading (% per cycle). Active material loading: 4.9 mg cm^{-2}, charge and discharge current: 0.042 mA cm^{-2} (0.05 C).

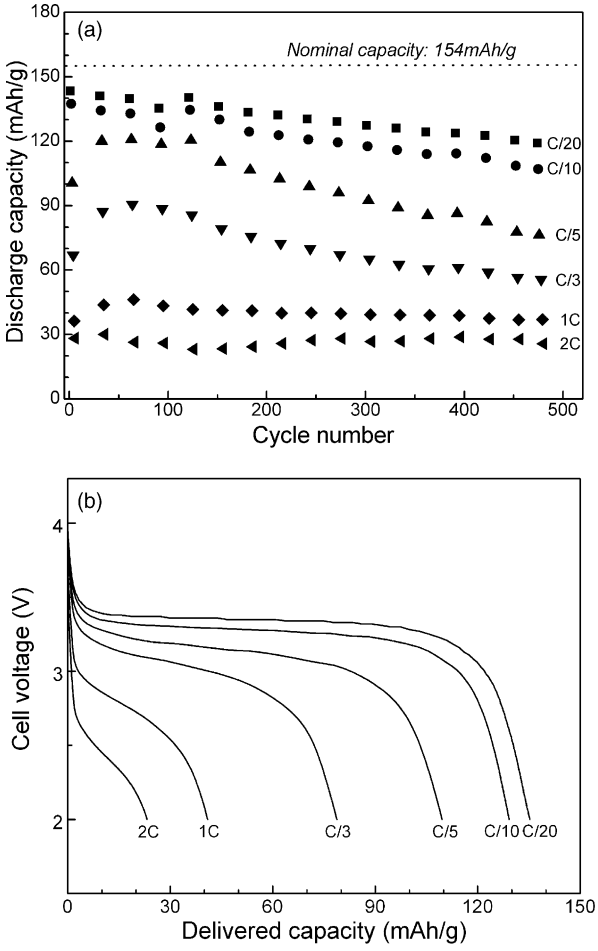

Fig. 3. (a) Rate performance and (b) voltage profiles (from the 151st cycle to 156th cycles) of a Li/P(EO)$_{20}$LiTFSI + IL/LiFePO$_4$ cell cycling at 40 °C at various discharge rates. Active material loading: 4.5 mg cm^{-2}. Charge rate was fixed at 0.038 mA cm^{-2} (0.05 C). Discharge rates and currents: 0.038 mA cm^{-2} (0.05 C), 0.076 mA cm^{-2} (0.1 C), 0.152 mA cm^{-2} (0.2 C), 0.251 mA cm^{-2} (0.33 C), 0.76 mA cm^{-2} (1 C) and 1.52 mA cm^{-2} (2 C).

with discharge currents ranging from 0.038 (0.05 C) to 1.52 mA cm^{-2} (2 C). The charge current was fixed at 0.038 mA cm^{-2} (0.05 C). In the first discharge at 0.05 C rate the active material utilization was about 95%, i.e., in full agreement with that of the cell reported in Fig. 1. Overall, the cell showed a very low capacity fading over approximately 500 cycles at different discharge rates. At intermediate discharge rates (from 0.2 to 1 C), however, the cell reached steady-state values of delivered capacity only after about 50 cycles. This behaviour has been consistently observed. However, the reason for the discharge capacity increase during the initial cycles is not clear. It may be due to the optimization of the electric contact between the cathode and the current collector or electrolyte or to an overall optimization of the cell due to the internal diffusion of the ionic liquid. Further investigations are ongoing to fully address this issue. Also observed in Fig. 3 is an increase of the delivered capacity, especially at low discharge rates, after the 100th cycle. The reason for this is known; it corresponds to a rest period of a few days during the cycle test.

The voltage profiles of the cell in a set of steady-state cycles (from the 151st discharge to the 156th discharge) at each current density are shown in Fig. 3b. The discharge curves at lower current densities resemble the typical voltage profiles of fully discharged Li/LiFePO$_4$ cells with a prolonged plateau in the 3.4–3.2 V range [20]. The ohmic drop of the cell on discharge was found to increase from about 0.48 V at the 1st cycle to about 0.58 V at the 229th cycle, in good agreement with the voltage plateau shift detected in the 0.05 C charge/discharge rate test (Figs. 1 and 2). However, the discharge capability of the LiFePO$_4$ cathode is seen to strongly depend upon the discharge rate. This is due to the increase of the electrolyte ohmic drop with increasing discharge current and the limited Li$^+$ cation diffusivity in the composite cathode [26]. Nevertheless, the cell was able to deliver about 24 and 15% of the theoretical capacity at high rate discharges (1 and 2 C) in, respectively, 14.1 and 4.5 min.

Fig. 4a shows the average delivered capacity (or active material utilization) of the Li/P(EO)$_{20}$LiTFSI + IL/LiFePO$_4$ cell as a function of current density. In order to exclude the initial anomalous behaviour observed in the medium and high rate discharges (see Fig. 3a) the average delivered capacities were calculated from the 150th cycle to the 500th cycle.

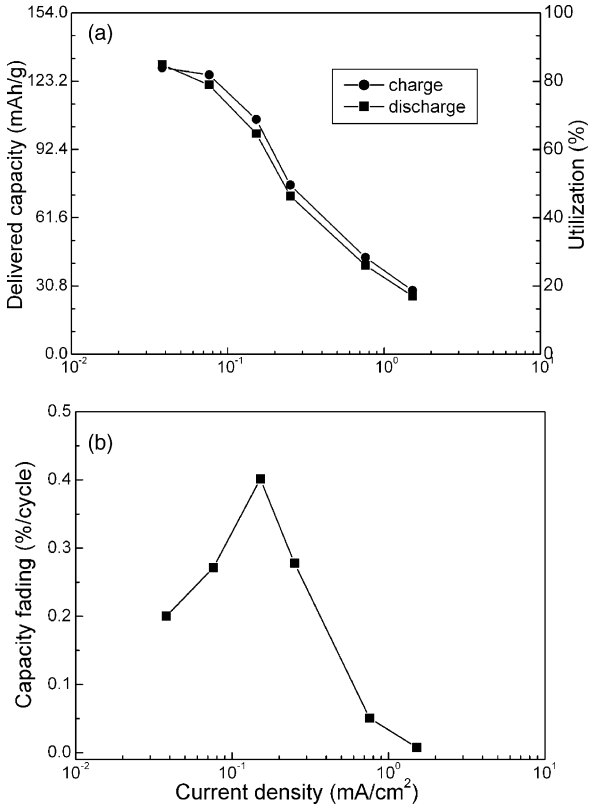

Fig. 4. (a) Discharge capacity and active material utilization and (b) average capacity fading after the 150th cycle as a function of discharge current for a Li/P(EO)$_{20}$LiTFSI + IL/LiFePO$_4$ cell cycling at 40 °C. These plots were obtained from the results reported in Fig. 3.

Between the 150th and the 500th cycles, the average active material utilization at 0.05 C was about 83% of the nominal capacity. However, the delivered capacity (active material utilization) exhibited a decline already at 0.2 C (0.152 mA cm^{-2}) and decreased sharply (below 43%) at 0.33 C rate (0.251 mA cm^{-2}). Such a steep decline has been previously observed in Li/P(EO)$_{20}$LiTFSI + $PYR_{14}TFSI/V_2O_5$ cells [7] and is due to a limitation of the polymer electrolyte transport properties. This rate limitation appears to be very severe when compared to commercial lithium-ion battery systems. However, a comparison with state of the art lithium metal-polymer electrolyte batteries [19], which operates at 60 °C, reveals that the introduction of the IL into PEO-based electrolytes results in a substantial technology improvement.

In Fig. 4a are also reports the average capacities charged by the same cell after the discharges at different rates. The data reported indicate a slight unbalance of the charge and discharge capacities. In practice, the cell was slightly overcharged after the discharges at all rates with the exception of the lowest rate (0.05 C). At this latter rate the charge efficiency ($Q_{charge}/Q_{discharge}$) is lower than unity. While it is expected to detect an average charge efficiency higher than 1 for a cell under continuous cycling (the cell fades on cycling thus the delivered capacity is lower than the charged capacity) it is very interesting to observe a charge efficiency lower than one at the lowest rate. In fact, it indicates that the charge step at 0.05 C rate is not able to fully recharge the battery when discharged at the same C rate. This evidence indicates that part of the fading observed in the cell tested at constant charge/discharge rate (see Fig. 2) is due to its incomplete recharge.

Fig. 4b shows the average capacity fading of the Li/P(EO)$_{20}$LiTFSI + IL/$LiFePO_4$ cell as a function of current density. As for the average delivered capacity, the fading in the high rate cycles has been evaluated from the 150th cycle and on. This procedure was used because including the data of the initial 150 cycles resulted in a capacity increase (instead of capacity fading) for the higher rate discharges. In addition, we have verified that the calculations for the lower discharge rates were not affected by not considering the initial 150 cycles (the slope of the 0.1 and 0.05 C does not change substantially before and after the 150th cycle). Also, it should be considered that the fading values reported in Fig. 4b are calculated with respect to the number of cycles at each specific discharge rate which is only 1/6 of the overall number of cycles. The average capacity fading at the different discharge rates calculated versus the total number of cycles is reported in Table 1.

At a glance the average capacity fading as a function of the current density reported in Fig. 4b shows a bell-like behaviour. It increases from 0.2% per cycle at a 0.05 C (0.038 mA cm^{-2}) rate to a maximum of 0.4% per cycle at a 0.2 C rate (0.152 mA cm^{-2}). At higher rate, the fading decreased sharply down to 0.05% at a 1 C rate (0.76 mA cm^{-2}) and approaching 0 at 2 C rate (1.52 mA cm^{-2}). The same trend is obviously observed in the data reported in Table 1 where the fading is reported versus the overall number of cycles. However, the values are much lower. The capacity fading for the discharges at 0.05 C rate is, with this calculation, lower than 0.035% per cycle. This value is lower than that detected in the constant rate charge/discharge test (0.056% per cycle, see Fig. 2). Such a lower fading is, at least partly due to the fact that in the multi-rate test the cell is fully recharged after the high rate cycles. As a matter of fact, the cell showed a charge efficiency ($Q_{charge}/Q_{discharge}$) always higher than unity (see Fig. 4a) at high discharge rates.

Table 1
Overall capacity fading versus discharge rate of a Li/P(EO)$_{20}$LiTFSI + IL/$LiFePO_4$ cell cycling at 40 °C evaluated after 500 cycles

Discharge rate (C)	Capacity fading	
	mAh g^{-1} cycle	% per cycle
0.05	0.051	0.033
0.1	0.064	0.042
0.2	0.051	0.033
0.33	0.024	0.016
1	0.023	0.015
2	0.005	0.004

The data were obtained from the results reported in Fig. 3.

Summarizing, the polymer electrolyte Li/$LiFePO_4$ (laboratory made) batteries incorporating the IL have a very stable cycling behaviour for about 500 cycles with only a very moderate capacity fading (<0.06% cycle^{-1}). Other research works have demonstrated that even higher capacity fadings in $LiFePO_4$ batteries are due to the formation of cracks in the $LiFePO_4$ particles [24] and structural or physical degradation of the electrodes [26].

The cycle performance of two cells cycled at moderate rates over 100% DOD at 40 °C is shown in Fig. 5. In the

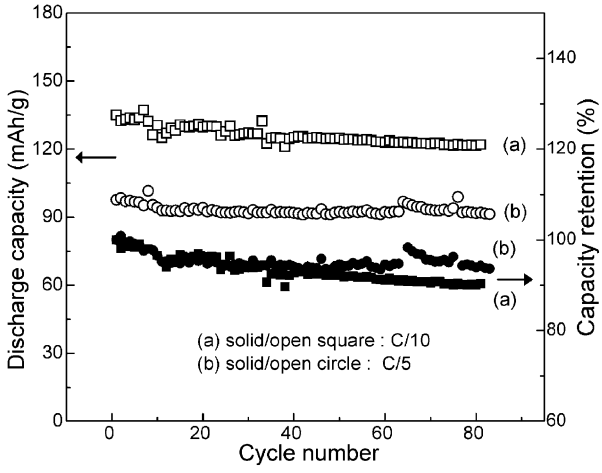

Fig. 5. Evolution of the delivered capacity and capacity retention of a Li/P(EO)$_{20}$LiTFSI + IL/$LiFePO_4$ cell upon cycling at high rate at 40 °C. Active material loading: (a) 3.8 and (b) 3.2 mg cm^{-2}. Charge current: (a) 0.065 (0.1 C) and (b) 0.055 (0.1 C) mA cm^{-2}. Discharge current: (a) 0.065 (0.1 C) and (b) 0.11 mA cm^{-2} (0.2 C).

first cycle at charge/discharge rate of 0.1 and 0.2 C, the cells delivered, respectively, 135 and 98 mAh g^{-1} corresponding to 87.7 and 63.7% of the active material's nominal capacity. Both cells showed good capacity retention on cycling. After 80 full charge/discharge cycles, the cells retained about 90 and 94% of the initial capacity at a 0.1 and 0.2 C rate, respectively. The cycling behaviour was very stable with a capacity fading of about 0.1% (0.161 mAh g^{-1} per cycle) and 0.05% (0.085 mAh g^{-1} per cycle) at a 0.1 and 0.2 C rate, respectively, which was close to that (0.06%) of the cell at a 0.05 C rate shown in Fig. 2. From the cycling performance at various rates, it is found that the $LiFePO_4$ cathode has an excellent cycle performance in the polymer electrolyte consisting of a conventional PEO-LiX electrolyte with added IL at moderate C rates and temperature.

The battery performance upon faster charge/discharge cycles at 40 °C was also investigated. Fig. 6 shows the cycling behaviour of a cell charged in constant current–constant voltage (CC–CV) conditions and discharged in constant current (0.33 C) conditions. The charge half-cycle was composed of a first step in which the cell was charged at a 0.33 C rate up to 4 V followed by a second step in which the voltage was kept constant at 4 V until the current flowing decreased to one tenth of the initial value (corresponding to 0.033 C). As shown in Fig. 6a, the full charge/discharge cycle averaged about 4.9 h with about 3.0 h during charge and 1.9 h during discharge. In the first discharge, the cell delivered 90 mAh g^{-1} corresponding to an active material utilization of about 59%. The evolution of the voltage and current profiles clearly indicates that the capacity delivered by the cell is limited by the charging process during which the cell voltage very quickly reaches the upper limit (4 V) in the galvanostatic step (0.33 C). Most of the recharge (lithium cation deinsertion from $LiFePO_4$) takes place during the potentiostatic step. In the following discharge, the cell is able to deliver the entire capacity accumulated even if a substantial initial voltage drop (down to 3 V) is observed. The discharge ability of the cell is confirmed by the very high average cycle efficiency ($Q_{discharge}/Q_{charge}$) of 0.999. The delivered capacity is very similar to that obtained in the galvanostatic discharge reported in Fig. 3, even if in the latter case the cell was charged at a much lower rate (0.05 C).

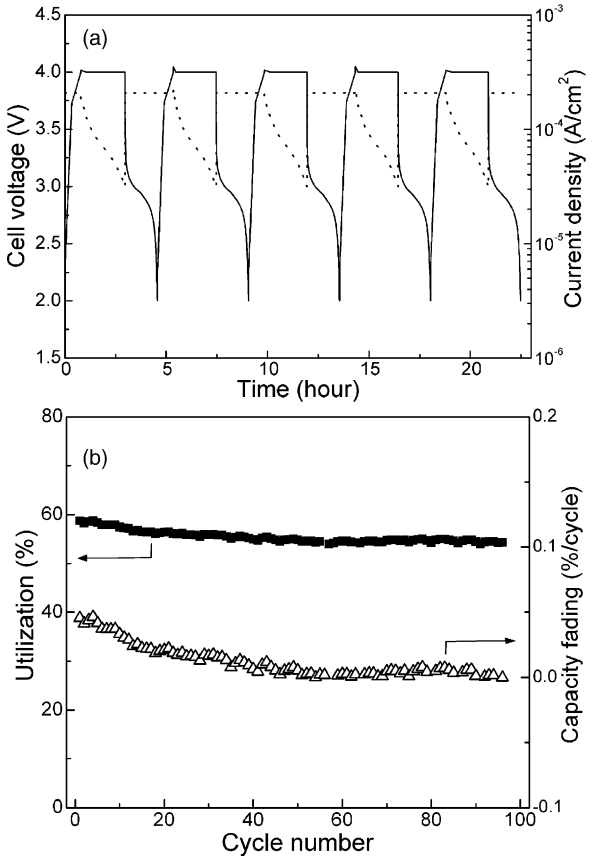

Fig. 6. Performance of a Li/P(EO)$_{20}$LiTFSI + IL/$LiFePO_4$ cell upon fast charge/discharge cycling at 40 °C. (a) Cell voltage (solid line) and current (dotted line) profiles during the initial cycles and (b) evolution of the active material utilization and capacity fading upon extended cycling. Active material loading: 3.71 mg cm^{-2}; charge: constant current (0.21 mA cm^{-2}, 0.33 C) + constant voltage (4 V until I ≥ 0.02 mA cm^{-2}), discharge current: 0.21 mA cm^{-2} (0.33 C).

Upon cycling (Fig. 6b), the cell retained about 93% of the initial capacity (90 mAh g^{-1}) after 100 cycles with a corresponding capacity fading of about 0.03% per cycle in a good agreement with that obtained in the discharge tests at 0.05 and 0.2 C rates mentioned earlier.

4. Conclusions

The solid-state Li/$LiFePO_4$ batteries based on the P(EO)$_{20}$LiTFSI + PYR$_{13}$TFSI polymer electrolyte reported in this work showed an excellent delivered capacity and cycle performance at a moderate rate (0.05 C) and temperature (40 °C). The active material utilization averaged over 500 cycles exceeded 76 and 43% on discharges at 0.1 and 0.33 C, respectively. More importantly, the charge and discharge efficiencies approached unity almost independently of the rate. Finally, no dendritic growth of lithium has been observed due to the moderate operating temperature and the high molecular weight of the polymer (PEO) used. To the best of our knowledge, no other lithium metal solvent-free polymer electrolyte battery has been reported which operates at 40 °C with such an exceptional performance. The introduction of new ILs is expected to allow the realization of improved batteries with practical operation at room temperature.

Acknowledgements

This research was financially supported by MURST. J.H.S. and W.A.H. gratefully acknowledge the postdoctoral fellowship programs of the Italian Foreign Ministry and the NSF International Research Fellowship Program (IRFP 0202620), respectively.

References

[1] J.M. Tarascon, M. Armand, Nature 414 (2001) 359.
[2] S. Chintapalli, R. Frech, Solid State Ionics 86–88 (1996) 341.
[3] L.R.A.K. Bandara, M.A.K.L. Dissanayake, B.-E. Mellander, Electrochim. Acta 43 (1998) 1447.
[4] J.H. Shin, W.A. Henderson, S. Passerini, Electrochem. Commun. 5 (2003) 1016.
[5] J.H. Shin, W.A. Henderson, S. Passerini, Electrochem. Solid-State Lett. 8 (2005) A125.
[6] J.H. Shin, W.A. Henderson, S. Passerini, J. Electrochem. Soc. 152 (2005) A978.
[7] J.-H. Shin, W.A. Henderson, G.B. Appetecchi, F Alessandrini, S. Passerini, Electrochim. Acta 50 (2005) 3859.
[8] J. Fuller, A.C. Breda, R.T. Carlin, J. Electroanal. Chem. 459 (1998) 29.
[9] H. Sakaebe, H. Matsumoto, Electrochem. Commun. 5 (2003) 594.
[10] A. Lewandowski, A. Swiderska, Solid State Ionics 169 (2004) 21.
[11] C.L. Hussey, Pure Appl. Chem. 60 (1998) 1763.
[12] A.A. Fannin, L.A. King, J.A. Levisky, J.S. Wilkes, J. Phys. Chem. 88 (1984) 2609.
[13] N. Papageorgiou, Y. Athanassov, M. Armand, P. Bonhôte, H. Pettersson, A. Azam, M. Grätzel, J. Electrochem. Soc. 143 (1996) 3009.
[14] V.R. Koch, L.A. Dominey, C. Nanjundiah, M.J. Ondrechen, J. Electrochem. Soc. 143 (1996) 798.
[15] Y.S. Fung, R.Q. Zhou, J. Power Sources 81 (1999) 891.
[16] H. Matsumoto, M. Yanagida, K. Tanimoto, M. Nomura, Y. Kitagawa, Y. Miyazaki, Chem. Lett. 29 (2000) 922.
[17] P. Bonhôte, A.P. Dias, M. Armand, N. Papageorgiou, K. Kalyanasundaram, M. Grätzel, Inorg. Chem. 35 (1996) 1168.
[18] D.R. MacFarlane, P. Meakin, J. Sun, N. Amini, M. Forsyth, J. Phys. Chem. B 103 (1999) 4164.
[19] D. Linden, T.B. Reddy (Eds.), Handbook of Batteries, 3rd ed., McGraw-Hill, 2002, Chapter 34.
[20] G.B. Appetecchi, J. Hausson, B. Scrosati, F. Croce, F. Cassel, M. Salomon, J. Power Sources 124 (2003) 246.
[21] M. Takahashi, S. Tobishima, K. Takei, Y. Sakurai, J. Power Sources 97–98 (2001) 508.
[22] P.P. Prosini, M. Carewska, S. Scaccia, P. Wisniewski, S. Passerini, M. Pasquali, J. Electrochem. Soc. 149 (2002) A886.
[23] S. Scaccia, M. Carewska, A. Di Bartolomeo, P.P. Prosini, Thermochim. Acta 383 (2002) 145.
[24] D. Wang, X. Wu, Z. Wang, L. Chen, J. Power Sources 140 (2005) 125.
[25] P.P. Prosini, D. Zane, M. Pasquali, Electrochim. Acta 46 (2001) 3517.
[26] J.P. Shim, K.A. Striebel, J. Power Sources 119–121 (2003) 955.